Inorg. Chem. **2002**, *41*, 946–957

From Clusters to Ionic Complexes: Structurally Characterized Thallium Titanium Double Alkoxides

Timothy J. Boyle,* Cecilia A. Zechmann, Todd M. Alam, and Mark A. Rodriguez

Advanced Materials Laboratory, Sandia National Laboratories, 1001 University Boulevard SE, Albuquerque, New Mexico 87106

Cybele A. Hijar and Brian L. Scott

Los Alamos National Laboratories, CST-18, Chemical Science and Technology Division—X-ray Diffraction Laboratory, Los Alamos, New Mexico 87545

Received October 19, 2001

A series of sterically varied titanium alkoxides {$[Ti(OR)_4]_n$, $n = 4$, OR = OCH_2CH_3 (OEt); $n = 1$, $OCH(CH_3)_2$ (OPr^i); $n = 2$, $OCH_2C(CH_3)_3$ (ONep); $n = 1$, $OC_6H_3(CH_3)_2$-2,6 (DMP)} were reacted with a series of thallium alkoxides {$[Tl(OR)]_x$ ($x = 4$, OR = OEt, ONep; $n = \infty$, DMP)}. The resultant products of the $[Tl(\mu_3\text{-OEt})]_4$-modified $[Ti(OR)_4]_n$ (OR = OEt, OPr^i, ONep) were found by X-ray analysis to be $Tl_4Ti_2(\mu\text{-O})(\mu_3\text{-OEt})_8(OEt)_2$ (**1**), $Tl_4Ti_2(\mu\text{-O})(\mu_3\text{-OPr}^i)_5(\mu_3\text{-OEt})_3(OEt)_2$ (**2**), and $TlTi_2(\mu_3\text{-OEt})_2(\mu\text{-OEt})(\mu\text{-ONep})_2(ONep)_4$ (**3**), respectively. The reaction of $[Tl(\mu_3\text{-OEt})]_4$, 12HOEt, and $4[Ti(\mu\text{-ONep})ONep)_3]_2$ to generate **3** in a higher yield resulted in the isolation of $TlTi_2(\mu_3\text{-OEt})(\mu_3\text{-ONep})(\mu\text{-OEt})(\mu\text{-ONep})_2(ONep)_4$ (**4**). Compounds **1** and **2** possess an octahedral (Oh) arrangement of two Ti and four Tl metal atoms around a μ-O central oxide atom (the Tl–O distance is too long to be considered a bond). For both compounds, each Ti atom adopts a distorted Oh geometry with one terminal OEt ligand. The Tl atoms are formally 4-coordinated, adopting a distorted pyramidal geometry using four μ_3-OR (OR = OEt or OPr^i) ligands to complete their coordination sphere. The Tl atoms reside ~1.4 Å below the basal plane of oxygens. In contrast to these structures, both **3** and **4** utilize ONep ligands and display reduced oligomerization yielding trinuclear complexes without oxo formation. The two Ti cations are Oh, and the single Tl cation is in a formal distorted pyramidal (PYD) arrangement. If the lone pair of the Tl cations are considered in the geometry, each Tl adopts a square base pyramidal geometry. Two terminal ONep ligands are bound to each Ti with the remainder of the molecule consisting of μ_3- and μ-ONep ligands. The reaction of $[Tl(\mu_3\text{-ONep})]_4$ with two equivalents of $[Ti(\mu\text{-ONep})(ONep)_3]_2$ also led to the isolation of the homoleptic trinuclear complex $TlTi_2(\mu_3\text{-ONep})_2(\mu\text{-ONep})_3(ONep)_4$ (**5**) which is analogous in structure to the mixed ligand species of **3** and **4**. Each Ti is Oh coordinated with six ONep ligands, and the single Tl is PYD bound by ONep ligands. A further increase in the steric bulk of the pendant ligands, using $[Tl(\mu\text{-DMP})]_\infty$ and $[Ti(\mu\text{-ONep})(ONep)_3]_2$, resulted in a further decrease in the nuclearity yielding the dinuclear species $TlTi(\mu\text{-DMP})(\mu\text{-ONep})(DMP)(ONep)_2$ (**6**). For **6**, the two metals are bound by a μ-ONep and a μ-DMP ligand. The Tl metal center was solved in a bent geometry while the Ti adopted a distorted trigonal bipyramidal (TBP) geometry using three ONep and two DMP ligands to fill its coordination sphere. Further increasing the steric bulk of the ancillary ligands using $Ti(DMP)_4$ and $[Tl(\mu\text{-DMP})]_\infty$ led to the formation of $[Tl^+][^-(\eta^{2-3}\text{-DMP})Ti(DMP)_4]$ (**7**). The Ti metal center is in a TBP geometry, and the "naked" Tl cation resides unencumbered by solvent molecules but was found to have a strong π-interaction with four DMP ligands of neighboring $Ti(DMP)_5^-$ anions. For this novel set of compounds, ^{205}Tl NMR spectroscopy was used to investigate the solution behavior of these compounds. Multiple ^{205}Tl resonances were observed for the solution spectra of the crystalline material of **1**–**6**, and a broad singlet was observed for **7**. The large number of minor resonances noted for these compounds was attributed to sensitivity of the Tl cation based on small variations due to ligand rearrangement. However, the major resonance noted in the ^{205}Tl NMR solution spectra of **1**–**7** are in agreement with their respective solid-state structures.

Introduction

Mixed metal alkoxide (or "single-source") precursors to ceramic materials are of increasing interest for materials production because of the ease of handling, uniformity of processing, and controlled cation stoichiometry. Often a metathesis synthetic route[1−5] can be used involving alkali metal-derivatized metal alkoxides as templates to more complex oligomers (eqs 1−2). Unfortunately, the alkali metal

* To whom correspondence should be sent. E-mail: tjboyle@sandia.gov.

10.1021/ic0110833 CCC: $22.00
Published on Web 01/18/2002

does not always cleanly transfer as written (eq 2). In an effort to understand the various influences on the metathesis system, the structural aspects of these alkali metal-derivatized titanium alkoxides ($[ATi(OPr^i)_5]_n$ where A = Li, Na, K and OR = $OCHMe_2$ (OPr^i), OCH_2CMe_3 (ONep)) were investigated. The OPr^i derivatives were found to be molecular for the smaller alkali metal and polymeric for the larger congeners: $[ATi(OPr^i)_5]_n$, [A = Li ($n = 2$), Na ($n = \infty$), K ($n = \infty$)].[6] Structurally, it has been determined that the use of the ONep ligand reduces the oligomerization of the final product.[7−14] For the analogous $[ATi(ONep)_5]_2$ species, tetranuclear structures were isolated, independent of the alkali metal introduced.[11] However, on the basis of structural considerations, the alkali metals of these $[ATi(OR)_5]_n$ compounds were unavailable for metathesis reactions.

$$M(OR)_x + AOR \rightarrow \text{“}AM(OR)_{x+1}\text{”} \quad (1)$$

$$y\text{“}AM(OR)_{x+1}\text{”} + M'Cl_y \xrightarrow{-yACl} \text{“}M'[M(OR)_{x+1}]_y\text{”} \quad (2)$$

To circumvent this problem, a more accessible cation was desired. The similarity in the unipositive Tl^+ ion with K^+ in both cation size and chemistry is well-documented;[15] however, the electronegativity of Tl (1.62) is substantially increased in comparison to K (0.8) and the other alkali metals [Li(1.0); Na(0.9)].[16] This suggests, as has been found, that Tl-modified transition metal complexes should exist as “salts”.[15] A Tl salt of a particular transition metal could allow for a cation that is more amenable to metathesis reactions. The structures of thallium alkoxides ($[Tl(OR)]_x$) for the lower alkoxides [OCH_2CH_3 (OEt); OPr^i; $OCMe_3$ (OBu^t)] have been found to adopt cubane structures based upon ^{203,205}Tl NMR and molecular weight determinations.[17,18] Recently, we have reported the structures of $[Tl(\mu_3\text{-ONep})]_4$ and $[Tl(\mu\text{-OAr})]_\infty$ [OAr = $OC_6H_3(Me)_2$-2,6 (DMP); $OC_6H_3(CHMe_2)_2$-2,6 (DIP)].[19] These well-characterized $[Tl(OR)]_x$ species were, therefore, available to us to initiate the synthesis of metathesis intermediates.

We chose to investigate double alkoxides of Ti because of the ubiquity of this cation in complex ceramic materials. The structures of the $[Ti(OR)_4]_n$ are well-known and have been identified as the tetrameric species $[Ti_2(\mu_3\text{-OR})(\mu\text{-OR})_2(OR)_3]_2$ (where OR = OMe or OEt) in the solid state.[20,21] Through the introduction of the more sterically demanding ONep ligand, we isolated the novel dinuclear species $[Ti(\mu\text{-ONep})(ONep)_3]_2$.[8] Therefore, because we possessed two well-characterized families of metal alkoxides that could be used in a metathesis synthesis process (eq 3a,b), we were in an ideal position to investigate the synthesis and characterization of Tl/Ti double alkoxides ($TlTi(OR)_5$) for potential use as templates to more complex metal alkoxides.

$$1/n[Ti(OR)_4]_n + 1/x[Tl(OR)]_x \rightarrow TlTi(OR)_5 \quad (3a)$$

$$TlTi(OR)_5 + MCl_y \rightarrow MTi(OR)_5Cl_{y-1} + TlCl \quad (3b)$$

This report details the synthesis, characterization, and subsequent manipulation of the structures of a series of $TlTi(OR)_5$. The resultant products of eq 3a were identified as $Tl_4Ti_2(\mu\text{-O})(\mu_3\text{-OEt})_8(OEt)_2$ (**1**), $Tl_4Ti_2(\mu\text{-O})(\mu_3\text{-OPr}^i)_5(\mu_3\text{-OEt})_3(OEt)_2$ (**2**), $TlTi_2(\mu_3\text{-OEt})_2(\mu\text{-OEt})(\mu\text{-ONep})_2(ONep)_4$ (**3**), $TlTi_2(\mu_3\text{-OEt})(\mu_3\text{-ONep})(\mu\text{-OEt})(\mu\text{-ONep})_2(ONep)_4$ (**4**), $TlTi_2(\mu_3\text{-ONep})_2(\mu\text{-ONep})_3(ONep)_4$ (**5**), $TlTi(\mu\text{-DMP})(\mu\text{-ONep})(DMP)(ONep)_2$ (**6**), and $[Tl^+][^-(\eta^{2-3}\text{-DMP})Ti(DMP)_4]$ (**7**). The solid-state behaviors of compounds **1**−**7** were determined by a number of methods including single-crystal X-ray diffraction experiments. The solution state properties of these compounds were also investigated using multinuclear NMR (^{1}H, ^{13}C, ^{205}Tl). The details of the synthesis and characterization of these compounds are reported below.

Experimental Section

All reactions were performed under a dry, inert atmosphere, using standard Schlenk, vacuum line, and glovebox techniques. Solvents were dried and freshly distilled immediately prior to use as previously described.[6,8] The following compounds were used as received (Aldrich): $[Tl(OEt)]_4$, HONep, and H-DMP. $Ti(OEt)_4$ (80% in HOEt, Aldrich) and $Ti(OPr^i)_4$ were vacuum distilled immediately prior to use. The following compounds were prepared as reported in the literature: $[Tl(\mu_3\text{-ONep})]_4$,[19] $[Tl(\mu\text{-OAr})]_\infty$,[19] and $[Ti(\mu\text{-ONep})(ONep)_3]_2$.[8] $Ti(DMP)_4$ was isolated from the heated reaction of $Ti(OPr^i)_4$ with an excess of H-DMP followed by vacuum distillation of the resultant volatile material.[22]

FT-IR spectral data were obtained on a Bruker Vector 22 spectrometer using KBr pellets pressed and handled under an atmosphere of flowing nitrogen. Elemental analysis was performed on a Perkin-Elmer 2400 CHN-S/O elemental analyzer. Solution

(1) Bradley, D. C.; Mehrotra, R. C.; Gaur, D. P. *Metal Alkoxides*; Academic Press: New York, 1978.
(2) Hubert-Pfalzgraf, L. G. *New. J. Chem.* **1987**, *11*, 663.
(3) Bradley, D. C. *Chem. Rev.* **1989**, *89*, 1317.
(4) Caulton, K. G.; Hubert-Pfalzgraf, L. G. *Chem. Rev.* **1990**, *90*, 969.
(5) Chandler, C. D.; Roger, C.; Hampden-Smith, M. J. *Chem. Rev.* **1993**, *93*, 1205.
(6) Boyle, T. J.; Bradley, D. C.; Hampden-Smith, M. J.; Patel, A.; Ziller, J. W. *Inorg. Chem.* **1995**, *34*, 5893.
(7) Boyle, T. J.; Alam, T. M.; Dimos, D.; Moore, G. J.; Buchheit, C. D.; Al-Shareef, H. N.; Mechenbier, E. R.; Bear, B. R. *Chem. Mater.* **1997**, *9*, 3187.
(8) Boyle, T. J.; Alam, T. M.; Mechenbeir, E. R.; Scott, B.; Ziller, J. W. *Inorg. Chem.* **1997**, *36*, 3293.
(9) Boyle, T. J.; Pedrotty, D. M.; Scott, B.; Ziller, J. W. *Polyhedron* **1997**, *17*, 1959.
(10) Boyle, T. J.; Alam, T. M.; Tafoya, C. J.; Scott, B. L. *Inorg. Chem.* **1998**, *37*, 5588.
(11) Boyle, T. J.; Alam, T. M.; Tafoya, C. J.; Mechenbeir, E. R.; Ziller, J. W. *Inorg. Chem.* **1999**, *38*, 2422.
(12) Boyle, T. J.; Clem, P. G.; Rodriguez, M. A.; Tuttle, B. A.; Heagy, M. D. *J. Sol-Gel Sci. Technol.* **1999**, *16*, 47.
(13) Boyle, T. J.; Gallegos, J. J., III.; Pedrotty, D. M.; Mechenbier, E. R.; Scott, B. L. *J. Coord. Chem.* **1999**, *47*, 155.
(14) Boyle, T. J.; Tyner, R. P.; Alam, T. M.; Scott, B. L.; Ziller, J. W.; Potter, B. G. J. *J. Am. Chem. Soc.* **1999**, *121*, 12104.
(15) Cotton, F. A.; Wilkinson, G. *Advanced Inorganic Chemistry*, 5th ed.; John Wiley & Sons: New York, 1988.
(16) Douglas, B.; McDaniel, D. H.; Alexander, J. J. *Concepts and Models of INORGANIC CHEMISTRY*, 2nd ed.; John Wiley & Sons: New York, 1965.
(17) Maroni, V. A.; Spiro, T. G. *Inorg. Chem.* **1968**, *7*.
(18) Burke, P. J.; Matthews, R. W.; Gillies, D. G. *J. Chem. Soc., Dalton Trans.* **1980**, 1439−1442.
(19) Zechmann, C. A.; Boyle, T. J.; Pedrotty, D. M.; Alam, T. M.; Lang, D. P.; Scott, B. L. *Inorg. Chem.* **2001**, *40*, 2177.
(20) Ibers, J. A. *Nature (London)* **1963**, *197*, 686.
(21) Wright, D. A.; Williams, D. A. *Acta Crystallogr., Sect. B* **1968**, *24*, 1107.
(22) Waratuke, S. A.; Thorn, M. G.; Fanwick, P. E.; Rothwell, A. P.; Rothwell, I. P. *J. Am. Chem. Soc.* **1999**, *121*, 9111.

NMR spectra were obtained using a 5 mm BB solution probe: ^{1}H (400.1 MHz) and ^{13}C{^{1}H} (100.6 MHz). High-resolution solution ^{205}Tl NMR spectra were obtained on a Bruker DMX400 at 230.9 MHz. All spectra were obtained on a specially tuned 5 mm Tl-{^{1}H} probe, using single pulse excitation and a 1 s recycle delay. The ^{205}Tl spectra were referenced to 0.001 M Tl(NO_3) in D_2O ($\delta = 0.0$ ppm).

General. Because of the similarity of the syntheses of **1**−**7**, a general description is supplied with variations noted in the individual sections. To a stirring solution of the desired $[Tl(OR)]_x$ in toluene, the appropriate $[Ti(OR)_4]_n$ was added via pipet or by slow addition of the powder. The resultant clear mixture was allowed to stir overnight, concentrated by rotary evaporation, and then cooled at −35 °C until crystals formed (∼24 h).

$Ti_2Tl_4(O)(OEt)_{10}$ (1). Reagents used: $[Ti(OEt)_4]_4$ (0.60 g, 2.63 mmol), $[Tl(OEt)]_4$ (1.30 g, 5.22 mmol). Crystalline yield: 0.54 g (30% based on Tl). FT-IR (KBr, cm^{-1}): 2951(s), 2905(w), 2841-(m), 1441(m), 1368(m), 1142(s), 1095(m), 1054(s), 964(w), 919-(w), 891(m), 654(s), 534(s). ^{1}H (400 MHz, toluene-d_8): δ 4.39(3.5 H, br mult, OCH_2Me), 4.17(1.0 H, br s, OCH_2Me), 1.29(7.0 H, mult, OCH_2*Me*). ^{13}C{^{1}H} (100.5 MHz, toluene-d_8): δ 71.3, 68.1, 65.5, 59.2 (O*C*H_2Me), 29.4, 27.3, 22.9 (OCH_2*Me*). ^{205}Tl(230.9 MHz, toluene-d_8): δ 1506, 1503, 1486, 1477(major), 1419, 1401. Anal. Calcd for $C_{20}H_{50}O_{11}Ti_2Tl_4$: C, 17.41; H, 3.65. Found: 17.61, C; 3.48, H.

$Ti_2Tl_4(O)(OPr^i)_5(OEt)_5$ (2). Reagents used: $Ti(OPr^i)_4$ (1.00 g, 3.52 mmol), $[Tl(OEt)]_4$ (1.75 g, 3.52 mmol), and ∼10 mL of toluene. FT-IR (KBr, cm^{-1}): 2951(s), 2915(m), 2856(m), 1446-(m), 1369(m), 1353(m), 1160(s), 1140(s), 1118(m), 1095(s),1055-(m), 1049(m), 958(s), 891(w), 826(w), 632(s), 542(m), 468(s), 420(w). ^{1}H(400 MHz, toluene-d_8): δ 5.32(1.0H, br s), 4.92(1.0H, br s), 4.47(2.3H, br s), 1.42(sh), 1.31(18.2H, br s). ^{13}C{^{1}H}(100.5 MHz, toluene-d_8): δ 76.7, 74.4, 66.2(O*C*HMe_2, O*C*H_2CH_3), 28.2, 27.3(OCH*Me*$_2$, OCH_2*C*H_3). ^{205}Tl(230.9 MHz, toluene-d_8): δ 2319, 2271, 2224, 1570, 1523(major), 1497, 1494, 1484. Anal. Calcd for $C_{26}H_{62}O_{11}Ti_2Tl_4$: C, 21.33; H, 4.27. Found: C, 20.94; H, 4.00.

$Ti_2Tl(OEt)_3(ONep)_6$ (3). Synthesis A. Reagents used: $[Ti-(ONep)_4]_2$ (1.00 g, 2.52 mmol), $[Tl(OEt)]_4$ (0.325 g, 1.26 mmol), and ∼10 mL of toluene. FT-IR (KBr, cm^{-1}): 2951(s), 2905(w), 2865(m), 1478(m), 1392(m), 1360(m), 1094(s), 1058(s), 1022(s), 884(m), 750(w), 673(s), 637(m), 521(m), 478(m), 402(w). ^{1}H (400 MHz, toluene-d_8): δ 4.83(4.2H, br mult), 4.02(1.0H, s), 0.95, 0.86-(sh) (18.4H, br s). ^{13}C{^{1}H}(100.5 MHz, toluene-d_8): δ 86.7-(O*C*HMe_2, O*C*H_2CH_3), 34.4 (OCH_2*C*Me_3), 27.2, 26.7(OCH_2C*Me*$_3$, OCH_2*C*H_3). ^{205}Tl (230.9 MHz, toluene-d_8): δ 1426, 1203, 1378, 1372, 1358(major), 1332. Anal. Calcd for $C_{36}H_{81}O_9Ti_2Tl$: C, 45.13; H, 8.52. Found: 40.31, C; 7.34, H. Synthesis B. $[Ti(OEt)_4]_4$ (1.13 g, 4.95 mmol) and $[Ti(ONep)_4]_2$ (5.83 g, 7.35 mmol) were weighed into a Schlenk flask and dissolved with ∼20 mL of hexanes. The solution was allowed to sit overnight, and then $[Tl(OEt)]_4$ (0.70 mL, 9.9 mmol) was added. The resulting solution was refluxed overnight with no visible change. The reaction was allowed to cool and the solvent removed in vacuo. (It was necessary to heat under vacuum in a warm water bath for several hours to obtain a white powdery solid.) Yield: 9.1 g (96% based on Ti). X-ray quality crystals could be grown from a concentrated toluene solution. The unit cells of crystals grown from Method A or B were identical.

$TlTi_2(OEt)_2(ONep)_7$ (4). Reagents used: $[Ti(ONep)_4]_2$ (12 g, 15.2 mmol), $[Tl(OEt)]_4$ (3.78. 15.2 mmol), HOEt (1.39 g, 30.3 mmol), and ∼50 mL of toluene. Powder yield: 11.4 g (77.6%). ^{1}H(400 MHz, toluene-d_8): δ 4.44, 4.38(1H, mult), 1.53(0.54H, br s, OCH_2*Me*), 1.05(3.1H, s, OCH_2C*Me*$_3$). ^{13}C{^{1}H}(100.5 MHz, toluene-d_8): δ 86.8(OCH_2CMe_3), 67.1, 65.9(O*C*H_2Me), 34.5-(OCH_2CMe_3), 27.6(OCH_2C*Me*$_3$), 26.8(OCH_2*Me*). ^{205}Tl (230.9 MHz, toluene-d_8): δ 1373, 1358(major), 1333. Anal. Calcd for $C_{39}H_{87}O_9Ti_2Tl$: C, 46.83; H, 8.76. Found: 40.31, C; 7.34, H.

$TlTi_2(ONep)_9$ (5). Reagents used: $[Ti(ONep)_4]_2$ (2.06 g, 5.20 mmol), $[Tl(ONep)]_4$ (0.76 g, 2.6 mmol), and ∼10 mL of toluene. Solvent was partially removed and the remaining material redissolved in hot hexanes. Yield: 1.25 g (41% based on Tl). FT-IR (KBr, cm^{-1}): 2950(s), 2882(m), 2864(s), 2821(m), 2674(w), 1478-(m), 1392(m), 1359(m), 1090(sh, s), 1054(br s), 1022(s), 934(w), 917(w), 903(w), 751(w), 667(m), 644(m), 598(m), 479(w), 438-(w). ^{1}H(400 MHz, toluene-d_8): δ 4.58(1.0H, br s, OCH_2CMe$_3$), 4.35(1.7H, br s, OCH_2CMe$_3$), 1.52 (1.4H, br mult, OCH_2CMe$_3$), 1.05 (7.8H, s, OCH_2C*Me*$_3$). ^{13}C{^{1}H}(100.5 MHz, toluene-d_8): δ 86.3, 65.9(O*C*H_2CMe$_3$), 34.5(OCH_2*C*Me$_3$), 26.7(OCH_2C*Me*$_3$). ^{205}Tl (230.9 MHz, toluene-d_8): δ 1406, 1380, 1374, 1360(major), 1340. Anal. Calcd for $C_{45}H_{99}O_9Ti_2Tl$: C, 49.84; H, 9.20. Found: 43.02, C; 7.74, H.

$TlTi(DMP)_2(ONep)_3$ (6). Reagents used: $[Ti(ONep)_4]_2$ (1.01 g, 2.54 mmol), $[Tl(DMP)]_\infty$ (0.83 g, 2.55 mmol), and toluene added (∼12 mL). The reaction was warmed which formed a yellow precipitate. The mother liquor was decanted and dried. Yield: 0.832 g (43% based on Ti). X-ray quality crystals were grown by redissolving the yellow powder in toluene followed by slow evaporation. FT-IR (KBr, cm^{-1}): 2950(m), 2917(m), 2851(m), 1587(m), 1463(s), 1421(s), 1375(w), 1265(s), 1236(sh s), 1208(s), 1161(w), 1091(s), 1030(w), 863(s), 761(s), 736(w), 711(w), 630-(s), 579(s), 559(s), 490 (w), 451(m), 421(m). ^{1}H(400 MHz, toluene-d_8): δ 7.10−6.98(mult, $OC_6H_3(Me)_2$-2,6 and toluene-d_8), 6.99(mult, $OC_6H_3(Me)_2$-2,6 and toluene-d_8), 4.07(7.9 H, s, OCH_2CMe$_3$), 2.47-(12 H, s, OC_6H_3(*Me*)$_2$-2,6), 0.95(39.8 H, s, OCH_2C*Me*$_3$). ^{13}C{^{1}H}-(100.5 MHz, toluene-d_8): δ 86.4(O*C*H_2CMe$_3$), 34.3(OCH_2*C*Me$_3$), 27.0(OCH_2C*Me*$_3$), 19.0(OC_6H_3(*Me*)$_2$-2,6). ^{205}Tl(230.9 MHz, toluene-d_8): δ 1453, 1427, 1405, 1395, 1379, 1364, 1359(major), 1339-(major), 1333. Anal. Calcd for $C_{31}H_{51}O_5TiTl$: C, 49.25; H, 6.80. Found: 45.54, C; 8.02, H.

$TlTi(DMP)_5$ (7). Reagents used: $Ti(DMP)_4$ (1.95 g, 3.66 mmol), $[Tl(DMP)]_\infty$ (1.19 g, 3.64 mmol), and ∼10 mL of THF. The reaction mixture was heated (60 °C), allowed to cool, and concentrated and allowed to set. The crystals are a dark yellow color. Yield: 1.37 g (44%). FT-IR (KBr, cm^{-1}): 3391(br w), 2963(w), 2920(w), 2867-(w), 1459(m), 1419(m), 1262(s), 1234(m), 1211(m), 1089(br s), 1019(br m), 869(m), 798(m), 759(m), 714(m), 573(w), 542(w). ^{1}H-(400 MHz, toluene-d_8): δ 6.81(1H, br s, $OC_6H_3(CH_3)_2$)), 6.67-(0.69H, t, $OC_6H_3(CH_3)_2$), 2.24(s, 4.9 H, $OC_6H_3(CH_3)_2$). ^{13}C{^{1}H}-(100.5 MHz, toluene-d_8, partial): δ 18.4($OC_6H_3(CH_3)_2$). ^{203}Tl (228.9 MHz, toluene-d_8): δ 2034. Anal. Calcd for $C_{40}H_{45}O_5TiTl$: C, 55.99; H, 5.29. Found: 50.66, C; 4.77, H.

Crystal Structure Determination. For each sample, except **3**, a suitable crystal was mounted from a pool of Fluorolube HO-125 onto a thin glass fiber and then immediately placed under a liquid N_2 stream on a Bruker AXS diffractometer. Data collection parameters for all compounds are given in Table 1. The radiation used was graphite monochromatized Mo Kα radiation ($\lambda = 0.710\ 73$ Å). Lattice determination and data collection were carried out using SMART version 5.054 software.[23] Data reduction was performed using SAINT+ 5.02 software.[23] Absorption correction using SADABS[23] in SHELXTL 5.1[23] was carried out for all compounds. Structure solution, graphics, and preparation of publication materials were performed using SHELXTL.[23] After all non-hydrogen atoms

(23) The listed versions of SAINT, SMART, XSHELL, XPOW in SHELXTL, and SADABS Software from Bruker Analytical X-ray Systems Inc., 6300 Enterprise Lane, Madison, WI 53719, were used in analysis.

Table 1. Data Collection Parameters for **1**−**7**

	1	**2**	**3**	**4**	**5**	**6**	**7**
formula	$C_{32}H_{80}O_{16.5}Ti_3Tl_6$	$C_{25}H_{65}O_{11}Ti_2Tl_4$	$C_{36}H_{81}O_9Ti_2Tl$	$C_{39}H_{65}O_9Ti_2Tl$	$C_{45}H_{81}O_9Ti_2Tl$	$C_{31}H_{51}O_5TiTl$	$C_{40}H_{45}O_5TiTl$
fw	2098.88	1455.05	958.18	978.08	1066.28	755.99	858.03
temp (K)	293(2)	168(2)	203(2)	168(2)	168(2)	168(2)	168(2)
space group	monoclinic *P*2(1)/*c*	monoclinic P2(1)/n	monoclinic $P2_1/n$	monoclinic *P*2(1)/*c*	monoclinic *P*2(1)/*m*	monoclinic *P*2(1)/*c*	orthorhombic *Pna*2(1)
a (Å)	9.787(3)	9.8449(7)	11.0326(7)	13.370(10)	10.655(2)	12.1149(10)	17.1148(12)
b (Å)	31.811(9)	23.1985(16)	15.7498(8)	18.4303(14)	18.990(4)	15.2386913)	10.5537(7)
c (Å)	17.773(5)	18.5769(12)	27.834(2)	20.5757(16)	14.081(3)	19.3032916)	19.6490(13)
β (deg)	100.528(4)	101.0970(10)	100.891(1)	104.198(2)	105.117(4)	105.758(2)	
V (Å^3)	5440(3)	4163.4(5)	4749.3(5)	4895.8(6)	2750.6(1)	3429.7(5)	3549.1(4)
Z	4	4	4	4	2	4	4
D_{calcd} (Mg/m^3)	2.562	2.321	1.340	1.327	1.287	1.464	1.606
μ (MoKα) (mm^{-1})	18.169	15.834	3.754	3.644	3.299	4.958	4.802
R1[a] (%)	4.40	4.80	10.93	7.53	15.83	2.86	3.71
wR2[b] (%)	8.13	11.93	27.80	21.45	25.54	6.02	9.65
R1[a] (all data, %)	10.30	11.46	16.89	17.73	24.82	5.47	4.75
wR2[b] (all data, %)	9.96	13.84	31.18	25.85	46.42	6.59	10.05

[a] $R1 = \sum||F_o| - |F_c||/\sum|F_o| \times 100$. [b] $wR2 = [\sum w(F_o^2 - F_c^2)^2/\sum(w|F_o|^2)^2]^{1/2} \times 100$.

were identified, the hydrogen atoms were fixed in positions of ideal geometry, and the entire structure was refined within the XSHELL software.[23] These idealized hydrogen atoms had their isotropic temperature factors fixed at 1.2 or 1.5 times the equivalent isotropic *U* of the C atoms to which they were bonded. Individual differences in data collection, structure solution, and refinement are reported below.

The structure of each was solved using direct methods. This solution typically yielded the heavier atoms and some C atoms. Subsequent Fourier synthesis gave the remaining C atom positions. The H atoms were fixed in positions of ideal geometry and refined within the XSHELL software. These idealized H atoms had their isotropic temperature factors fixed at 1.2 or 1.5 times the equivalent isotropic *u* of the C atoms for which they were bonded.

$Ti_2Tl_4(O)(OEt)_{10}$ (1). The C atoms C(17), C(18), C(19), and C(20) (apical OEt ligands) were highly disordered and had to be modeled using SADI (same distance)[23] restraints on the C−C and C−O bond lengths of the OEt groups (SD 0.04 Å). Hence, the thermal ellipsoid plot presents only one of several orientations. The two molecules in the unit cell are essentially identical, but the second molecule does not display as large a disordering effect for the apical OEt groups off of the Ti atoms.

$Ti_2Tl_4(O)(OPr^i)_5(OEt)_5$ (2). This structure had significant disorder among the ligands resulting in multiple carbon sites with partial occupancies. Initial refinements indicated that the apical ligands best refined as disordered OEt groups. The O1−C1−C2/C2′ OEt was modeled by employing a simple disorder of the methyl carbon over two sites (C2 and C2′), each having $^1/_2$ occupancy. The O2 OEt was a little different in that it was best modeled with three possible orientations. The first orientation described by O2−C3−C4 accounts for $^1/_2$ of the OEt group. The balance of this OEt can be accounted for with the O2−C3′−C4′ and O2−C3′−C4″ ligands where C4′ and C4″ both have $^1/_4$ occupancy. These apical ligands make up two of the five total OEt groups within the structure.

The μ-ligands displayed disordering of OPr^i and OEt groups. This was indicated by a tendency of one methyl carbon in the ligand to refine as fully occupied while an additional methyl carbon (C′) site tended to prefer $^1/_2$ occupancy. An example of this is the O7−C14−C15/C15′ ligand. Here, the O7−C14−C15 accounts for a complete OEt ligand. However, the addition of a C15′ site at $^1/_2$ occupancy means that this ligand can be an OPr^i half of the time. This disordering was observed for additional μ-ligands as follows: O3−C5−C6/C6′, O4−C7−C8/C8′, O5−C9−C10/C10′, O8−C16−C17/C17′, and O9−C18−C19/C19′ where the C′ sites were fixed at $^1/_2$ occupancy. These disordered μ-OPr^i/μ-OEt groups accounted for three of the OPr^i and three of the OEt ligands in the structure. The O6−C11−C12/C13 and O10−C20−C21/C22 groups were refined as complete OPr^i groups and accounted for the final two OPr^i ligands in the molecule.

Because of the significant disorder, several additional restrictions were imposed during refinement. First, hydrogen atoms were left off of the structure. However, they were accounted for in the chemical formula based on five OPr^i and five OEt ligands per molecule. Second, SADI (same distance)[23] restraints were employed for all O−C bonds, restricting them all to be equivalent (SD 0.04 Å). Similarly, all C−C bonds were restrained with the SADI command to be equivalent (SD 0.04 Å).

$Ti_2Tl(OEt)_3(ONep)_6$ (3). A colorless, multifaceted block crystal was chosen from a pool of mineral oil and immediately placed on a Bruker P4/CCD/PC diffractometer that was cooled to 203 K using a Bruker LT-2 temperature device. The data were collected using a sealed, graphite monochromatized Mo Kα X-ray source. A hemisphere of data was collected using a combination of φ and ω scans, with 30 s frame exposures and 0.3 s frame widths. Data collection and initial indexing and cell refinement were handled using SMART[23] software. Frame integration and final cell parameter calculation were carried out using SAINT[23] software. The final cell parameters were determined using a least-squares fit to 9402 reflections. The data were corrected for absorption using the SADABS[23] program with no observation of any decay of reflection intensity.

The structure was solved in space group $P2_1/n$ using Patterson and difference Fourier techniques. The initial solution revealed the Ti, Tl, and the majority of all non-H atom positions. The remaining atomic positions were determined from subsequent Fourier synthesis. All H atom positions were fixed using the HFIX command in SHELXTL PC.[23] The C−H distances were fixed at 0.97 Å (methylene) or 0.96 Å (methyl). The hydrogen atom positions were refined using a riding model, with their isotropic temperature factors set to 1.2 times (methylene) or 1.5 times (methyl) the equivalent isotropic *U* of the carbon atom to which they were bound. The Tl atom was split over three positions. The site occupancy factors for these sites were tied to one for the refinement. The site occupancy

factors refined to approximately 0.681(3) for Tl(1), 0.281(2) for Tl(2), and 0.038(2) for Tl(3). The ONep groups were constrained as a rigid group owing to their disorder as seen in the difference map. The final refinement included anisotropic temperature factors on all non-hydrogen atoms. Structure solution, refinement, creation of publication tables, and graphics were performed using SHELXTL PC.[23]

Some of the OEt and ONep ligands were found to be disordered. The O2 OEt was found to have disordered terminal carbons and was modeled by placing $^1/_2$ occupied C atoms on C7 and C7′ sites. There were three ONep groups that displayed disorder. These were associated with O4, O5, and O6 oxygens. For the O4 ONep, there were two orientations for the ligand, O4−C10−C11−C12/C13/C14 and O4−C10′−C11−C12/C13′/C14′ where C10/C10′, C13/C13′, and C14/C14′ pairs were fixed at $^1/_2$ occupancy for individual carbon atoms. For the O5 ONep, there were two orientations for the ligand, O5−C15−C16−C17/C18/C19 and O5−C15−C16−C17′/C18′/C18′ where C17/C17′, C18/C18′, and C19/C19′ pairs were fixed at $^1/_2$ occupancy for individual carbon atoms. For the O6 ONep, there were again two orientations for the ligand, O6−C20−C21−C22/C23/C24 and O6−C20′-C21−C22′/C23′/C24 where C20/C20′, C22/C22′, and C23/C23′ pairs were fixed at $^1/_2$ occupancy for individual carbon atoms. Only isotropic displacement parameters were refined for the C atoms. Because of the severe disorder of the ligands, the H atoms were ignored in the solution but assumed in the stoichiometry. Additional Tl sites were observed, and the overall Tl content of 1.0 was distributed over these three sites as follows: Tl(1) occupancy = 0.90, Tl(1a) occupancy = 0.05, and Tl(1b) occupancy = 0.05.

$TlTi_2(\mu_3\text{-ONep})_2(\mu\text{-ONep})_3(ONep)_4$ (5). The structure of **5** possessed a high degree of structural disorder preventing full discussion of the final structure. For **5**, a mirror plane perpendicular to the *c*-axis bisects the structure through the two Ti atoms, one possible Tl site, and three ONep groups. The Tl cation was found to be distributed over three possible sites, with each site coordinating to different ONep ligands. This Tl disorder generated different O and C positions, and, hence, different ONep ligand orientations, depending on the presence/absence of the Tl cation over the three disordered locations. Further complicating the structure is the replication of the disorder across the mirror plane, thus magnifying structure defects by a factor of 2. Even with the high degree of disordering, it was possible to locate the ONep ligands extending from the central core of the molecule and refine the structure to an R1 = 0.1416 and wR2 = 0.2398. Because of the high degree of disorder and thus high R-values, the metrical data is not reliable, but the connectivity was unequivocally identified.

Results and Discussion

While Tl is highly toxic, in relatively small amounts,[24] it is reportedly an excellent complexing agent for halide atoms.[15] Therefore, we undertook the synthesis of $TlTi(OR)_5$ compounds (eq 3a) which would then be used as templates to additional mixed metal compounds (eq 3b). In this report, we detail the syntheses and characterization of a series of sterically varied $TlTi(OR)_5$, where we demonstrate the ability to generate Tl cations which have variable degrees of accessibility based on the choice of ligands.

Synthesis. The synthesis of compounds **1**−**7** involved the mixing of the various metal alkoxide precursors, exploiting their potential to oligomerize due to the large radius-to-charge ratio. The initial reactions investigated focused on the stoichiometric reaction between $1/n[Ti(OR)_4]_n$ and $1/x[Tl(OR)]_x$. Additional alterations in the stoichiometry increased yields but did not lead to the isolation of new products being formed. Thermal ellipsoid plots of the resultant products of these reactions, **1**−**7**, are shown in Figures 1−7, respectively.

Our initial syntheses utilized the commercially available species $[Tl(\mu_3\text{-OEt})]_4$ (an oil) and either $[Ti_2(\mu_3\text{-OEt})(\mu\text{-OEt})_2(OEt)_5]_2$ or $Ti(OPr^i)_4$ (an oil). The appropriate $[Tl(\mu_3\text{-OEt})]_4$ was dissolved in toluene, and $[Ti(OR)_4]_n$ was added via pipet. The mixture was stirred for 24 h to ensure that a complete reaction had occurred. During this time, no precipitates formed, and the solution remained clear and colorless. Heating of the solution was not attempted because of the predisposition of $[Tl(\mu_3\text{-OEt})]_4$ to decompose to Tl^0.[19] The solution was concentrated by rotary evaporation and cooled to −35 °C. After ∼1 day, X-ray quality crystals of each sample were obtained and solved as $Tl_4Ti_2(\mu\text{-O})(\mu_3\text{-OEt})_8(OEt)_2$ (**1**) or $Tl_4Ti_2(\mu\text{-O})(\mu_3\text{-OPr}^i)_5(\mu_3\text{-OEt})_3(OEt)_2$ (**2**).

Because of the encumbered nature of the Tl cations in these structures, the steric bulk of the pendant hydrocarbon chains of the various ligands was increased to generate more accessible Tl cations. The Ti precursors used were $[Ti(\mu\text{-ONep})(ONep)_3]_2$[8] and $Ti(DMP)_4$,[22] and the Tl precursors used were $[Tl(\mu\text{-ONep})(ONep)_3]_4$[19] and $[Tl(\mu\text{-DMP})]_\infty$.[19] The resultant products isolated from the various combinations of the parent alkoxides were identified as $TlTi_2(\mu_3\text{-OEt})_2(\mu\text{-OEt})(\mu\text{-ONep})_2(ONep)_4$ (**3**), $TlTi_2(\mu_3\text{-OEt})(\mu_3\text{-ONep})(\mu\text{-OEt})(\mu\text{-ONep})_2(ONep)_4$ (**4**), $TlTi_2(\mu_3\text{-ONep})_2(\mu\text{-ONep})_3(ONep)_4$ (**5**), $TlTi(\mu\text{-DMP})(\mu\text{-ONep})(DMP)(ONep)_2$ (**6**), and $[Tl^+][^-(\eta^{2-3}\text{-DMP})Ti(DMP)_4]$ (**7**).

Solid State. Crystals of **1**−**7** were dried in vacuo to yield the bulk powder that was used for the following analyses. The FT-IR data for **1**−**7** show stretches consistent with the appropriate ligands. The spectra of **1**−**6** have no stretches or bends in the 3000 cm^{-1} region which is most often associated with an OH stretch. This indicates there is no residual alcohol and the reaction was complete. For **7**, a sharp peak was present at 3391 cm^{-1} which may be a reflection of the ionic nature of **7** or the Tl−π-arene interaction as opposed to the presence of residual alcohol. The Tl−O stretches for **1**−**7** could not be discerned because of the complex nature of the M−O region. Elemental analyses of bulk samples of **1** and **2** were consistent with their solid-state structures. For **3**−**7**, the elemental analyses of the powder were considerably varied from acceptable analyses. For the ONep ligated species (**3**−**6**), the preferential loss of $[Ti(\mu\text{-ONep})(ONep)_3]_2$, which was found to be very volatile, may explain the unacceptable elemental analyses. It has been reported that $[Ti(\mu\text{-ONep})(ONep)_3]_2$ is an excellent MOCVD precursor,[25] and we have previously observed preferential loss of this moiety from other complex molecules upon warming.[26] Therefore, for **3**−**6**, the decomposition of the

(24) Labianca, D. A. *J. Chem. Educ.* **1990**, *67*, 1019.

(25) Gallegos, J. J. I.; Ward, T. L.; Boyle, T. J.; Francisco, L. P.; Rodriguez, M. A. *Chem. Vap. Deposition* **2000**, *6*, 21.

(26) Gallegos, J. J. I. Senior Thesis, Department of Nuclear and Chemical Engineering, University of New Mexico, Albuquerque, NM, 1999, unpublished.

Table 2. Select Bond Distances (Å) and Angles (deg) for **1**−**2**

Distances (Å)

	1		**2**	
Tl···Ti	Ti(1)···Tl(1)	3.437(3)	Tl(1)···Ti(1)	3.417(2)
	Ti(1)···Tl(2)	3.441(3)	Tl(2)···Ti(1)	3.437(2)
	Ti(1)···Tl(3)	3.419(3)	Tl(3)···Ti(1)	3.418(2)
	Ti(1)···Tl(4)	3.414(3)	Tl(4)···Ti(1)	3.472(19)
Ti−OR	Ti(1)−O(11)	1.772(10)	Ti(1)−O(1)	1.808(8)
	Ti(2)−O(10)	1.801(10)	Ti(2)−O(2)	1.827(8)
Tl−(μ_3-OR)	Tl(1)−O(2)	2.620(9)	Tl(1)−O(5)	2.680(8)
	Tl(1)−O(3)	2.622(10)	Tl(1)−O(4)	2.612(8)
	Tl(1)−O(8)	2.631(10)	Tl(1)−O(7)	2.687(8)
	Tl(1)−O(9)	2.645(10)	Tl(1)−O(10)	2.656(7)
Ti−(μ-OR)	Ti(1)−O(3)	1.985(10)	Ti(1)−O(3)	2.012(7)
	Ti(1)−O(5)	1.979(10)	Ti(10−O(4)	2.025(7)
	Ti(1)−O(7)	1.971(10)	Ti(1)−O(5)	1.991(8)
	Ti(1)−O(9)	1.981(10)	Ti(1)−O(6)	1.989(7)
Tl···(μ-O)	Tl(1)···O(1)	2.892	Tl(1)···O(11)	2.806(6)
	Tl(2)···O(1)	2.889	Tl(2)···O(11)	2.863(6)
	Tl(3)···O(1)	2.805	Tl(3)···O(11)	2.785(6)
	Tl(4)···O(1)	2.808	Tl(4)···O(11)	2.864(6)
Ti−(μ-O)	Ti(1)−O(1)	1.902(9)	Ti(1)−O(11)	1.921(7)
	Ti(2)−O(1)	1.896(9)	Ti(2)−O(11)	1.925(7)

Angles (Å)

	1		**2**	
Ti−(μ-O)−Ti	Ti(1)−O(1)−Ti(2)	176.9(6)	Ti(1)−O(11)−Ti(2)	178.0(4)
Tl−(μ_3-OR)−Tl	Tl(1)−O(2)−Tl(2)	101.5(3)	Tl(1)−O(4)−Tl(4)	98.5(3)
	Tl(1)−O(3)−Tl(2)	100.6(3)	Tl(1)−O(5)−Tl(3)	96.4(3)
	Tl(1)−O(8)−Tl(4)	99.8(3)	Tl(1)−O(7)−Tl(3)	97.1(3)
	Tl(1)−O(9)−Tl(4)	98.3(3)	Tl(1)−O(10)−Tl(4)	97.6(2)
Ti−(μ_3-OR)−Tl	Ti(1)−O(3)−Tl(1)	95.5(4)	Ti(1)−O(3)−Tl(2)	93.6(3)
	Ti(1)−O(3)−Tl(2)	94.7(3)	Ti(1)−O(3)−Tl(4)	95.5(3)
	Ti(1)−O(5)−Tl(2)	95.4(3)	Ti(1)−O(4)−Tl(1)	94.0(3)
	Ti(1)−O(5)−Tl(3)	94.0(4)	Ti(1)−O(4)−Tl(4)	94.0(3)
	Ti(1)−O(7)−Tl(3)	94.6(4)	Ti(1)−O(5)−Tl(1)	92.8(3)
	Ti(1)−O(7)−Tl(4)	93.5(4)	Ti(1)−O(5)−Tl(3)	93.7(3)
	Ti(1)−O(9)−Tl(1)	94.9(4)	Ti(1)−O(6)−Tl(2)	94.2(2)
	Ti(1)−O(9)−Tl(4)	93.2(4)	Ti(1)−O(6)−Tl(3)	92.3(2)
(μ_3-OR)−Tl−(μ_3-OR)	O(3)−Ti(1)−O(5)	89.6(4)	O(3)−Ti(1)−O(4)	88.0(3)
	O(3)−Ti(1)−O(7)	169.1(4)	O(3)−Ti(1)−O(5)	168.4(3)
	O(3)−Ti(1)−O(9)	88.3(4)	O(3)−Ti(1)−O(6)	90.2(3)
	O(5)−Ti(1)−O(7)	89.4(4)	O(4)−Ti(1)−O(5)	89.5(3)
	O(5)−Ti(1)−O(9)	169.1(4)	O(4)−Ti(1)−O(6)	169.2(3)
	O(7)−Ti(1)−O(9)	90.7(4)	O(5)−Ti(1)−O(6)	90.1(3)
(OR)−Ti−(μ-O)	O(11)−Ti(1)−O(1)	178.9(5)	O(1)−Ti(1)−O(11)	179.6(4)
(μ_3-OR)−Tl−(μ_3-OR)	O(2)−Tl(1)−O(3)	79.2(3)	O(4)−Tl(1)−O(5)	64.6(2)
	O(2)−Tl(1)−O(8)	64.6(3)	O(4)−Tl(1)−O(7)	115.5(2)
	O(2)−Tl(1)−O(9)	113.0(3)	O(4)−Tl(1)−O(10)	81.9(2)
	O(3)−Tl(1)−O(8)	112.8(3)	O(5)−Tl(1)−O(7)	82.4(2)
	O(3)−Tl(1)−O(9)	63.2(3)	O(5)−Tl(1)−O(10)	115.5(2)
	O(8)−Tl(1)−O(9)	81.1(3)	O(7)−Tl(1)−O(10)	64.2(2)
(μ_3-OR)−Tl−(μ_3-OR)	O(2)−Tl(1)−O(1)	56.67(2)	O(4)−Tl(1)−O(11)	58.22(2)
	O(3)−Tl(1)−O(1)	56.59(2)	O(5)−Tl(1)−O(11)	57.28(2)
	O(8)−Tl(1)−O(1)	56.25(2)	O(7)−Tl(1)−O(11)	57.33(2)
	O(9)−Tl(1)−O(1)	56.44(2)	O(10)−Tl(1)−O(11)	58.23(19)

thermally treated compounds may involve loss of "Ti(ONep)$_4$" which would lead to elemental analyses with lower C and H percentages than expected, as is observed. For **7**, the ionic nature of the precursor may also preferentially lead to preferential volatilization of the monomeric sterically hindered Ti(OAr)$_4$ complex.[22]

X-ray Structures. Table 1 lists the data collection parameters for **1**−**7**. Tables 2−4 list the metrical data for **1**−**2**, **4**, and **6**−**7**, respectively. Figures 1−7 are thermal ellipsoid plots of **1**−**7**, respectively. There are no reports of other TlTi(OR)$_5$ complexes available in the literature, and hence, there are no representative model compounds to use for comparison. However, the structures observed for these double alkoxides are reminiscent of other mixed metal species, and discussions of these compounds are included where appropriate.

Structural Arrangements. Compounds **1** and **2** were found to adopt similar hexanuclear $Tl_4Ti_2(O)(OR)_{10}$ arrangements (shown in Figures 1 and 2, respectively). For **2**, there is significant disorder noted between the OEt and OPr^i ligands. The μ-oxo atom is octahedrally (Oh) bound by four equatorial Tl and two axial Oh bound Ti atoms. The Tl···O distance is too great to formally be considered a bond, and thus, the oxo ligand only bridges between the Ti metal centers. The oxo ligand formed in metal alkoxide exchange reactions is often reported to be due to decomposition either

Table 3. Select Bond Distances (Å) and Angles (deg) for **4**

Distances (Å)

	4	
Tl···Ti	Tl(1a)···Ti(1)	3.544(7)
	Tl(1b)···Ti(1)	3.529(9)
	Tl(1a)···Ti(2)	3.400(8)
	Tl(1b)···Ti(2)	3.535(7)
Ti···Ti	Ti(1)···Ti(2)	3.039(6)
Tl−(μ_3-OR)	Tl(1)−O(1)	2.622(6)
	Tl(1)−O(2)	2.549(6)
Tl−(μ-OR)	Tl(1)−O(4)	2.760(7)
	Tl(1)−O(5)	2.691(7)
Ti−(μ_3-OR)	Ti(1)−O(1)	2.107(6)
	Ti(1)−O(2)	2.118(6)
	Ti(2)−O(1)	2.127(6)
	Ti(2)−O(2)	2.118(6)
Ti−(μ-OR)	Ti(1)−O(3)	2.064(6)
	Ti(2)−O(3)	2.052(6)
	Ti(1)−O(4)	1.879(6)
	Ti(2)−O(5)	1.885(7)
Ti−(OR)	Ti(1)−O(6)	1.811(6)
	Ti(1)−O(7)	1.784(6)
	Ti(2)−O(8)	1.787(6)
	Ti(2)−O(9)	1.830(6)

Angles (Å)

	4	
(μ_3-OR)−Ti−(μ_3-OR)	O(1)−Ti(1)−O(2)	69.4(2)
(μ_3−OR)−Ti−(μ-OR)	O(1)−Ti(1)−O(3)	73.3(2)
	O(1)−Ti(1)−O(4)	89.9(3)
	O(2)−Ti(1)−O(3)	75.5(2)
	O(2)−Ti(1)−O(4)	86.0(3)
(μ_3-OR)−Ti−(OR)	O(1)−Ti(1)−O(6)	95.0(3)
	O(1)−Ti(1)−O(7)	161.4(3)
	O(2)−Ti(1)−O(6)	163.7(3)
	O(2)−Ti(1)−O(7)	95.0(3)
(μ-OR)−Ti−(μ-OR)	O(3)−Ti(1)−O(4)	158.3(3)
(μ-OR)−Ti−(OR)	O(3)−Ti(1)−O(6)	95.8(3)
	O(3)−Ti(1)−O(7)	93.4(3)
	O(4)−Ti(1)−O(6)	99.3(3)
	O(4)−Ti(1)−O(7)	99.4(3)
(OR)−Ti−(OR)	O(6)−Ti(1)−O(7)	99.3(3)
(μ_3-OR)−Tl−(μ_3-OR)	O(1)−Tl(1)−O(2)	55.45(18)
(μ-OR)−Tl−(μ-OR)	O(4)−Tl(1)−O(5)	117.08(19)
(μ_3-OR)−Tl−(μ-OR)	O(1)−Tl(1)−O(4)	63.15(18)
	O(1)−Tl(1)−O(5)	63.13(19)
	O(2)−Tl(1)−O(4)	61.77(19)
	O(2)−Tl(1)−O(5)	62.0(2)
Ti(1)−(μ_3-OR)−Ti(2)	Ti(1)−O(1)−Ti(2)	91.7(2)
	Ti(1)−O(2)−Ti(2)	92.6(2)
Ti(1)−(μ_3-OR)−Ti(2)	Ti(1)−O(3)−Ti(2)	95.2(2)
Ti−(μ_3-OR)−Tl(1)	Ti(1)−O(1)−Tl(1)	94.0(2)
	Ti(2)−O(1)−Tl(1)	93.19(19)
	Ti(1)−O(2)−Tl(1)	95.8(2)
	Ti(2)−O(2)−Tl(1)	96.3(2)
Ti−(μ-OR)−Tl(1)	Ti(1)−O(4)−Tl(1)	95.2(3)
	Ti(2)−O(5)−Tl(1)	96.9(3)

of the alkoxy ligand or through adventitious water; however, the later argument is unlikely because of the absence of oxo formation in the synthesis of the other $TlTi(OR)_5$ species under identical conditions. The arrangements of **1** and **2** are similar to the structure observed for the double alkoxide $Zr_2K_4(O)(OPr^i)_{10}$ species. This compound was synthesized through the mixing of $KZr_2(OPr^i)_9$ and 3 equiv of $K(OPr^i)$[27] which is analogous to the preparation of **1** and **2**. For the K/Zr system, it was found that the oxide was formed through ligand decomposition[27] supporting the assumption that this is the source of the oxo for **1** and **2**. The Tl cations are formally 4-coordinated and adopt a distorted pyramidal geometry. Inclusion of the lone pair of electrons of the Tl atoms in the geometrical considerations leads to each Tl cation adopting a distorted square base pyramidal (SBP) geometry. The Tl atoms reside on average 1.43 Å (1.44 Å, **1**; 1.42 Å, **2**) above the base of the pyramid. Each Ti possesses a terminal OEt ligand and is bound to two of the equatorial Tl atoms by one of the eight μ_3-OR ligands (**1**, OEt; **2**, OPr^i). As mentioned in previous reports, the ONep derivatives appear to adopt smaller nuclearity compounds in comparison to other short chain alkoxides.[7−14] Therefore, the ONep ligand was introduced to increase the steric bulk around the Tl metal center which should make it more accessible for metathesis reactions. For the synthesis of **3**−**5**, $[Ti(\mu\text{-ONep})(ONep)_3]_2$[8] was used, and their thermal ellipsoid plots are shown in Figures 3−5, respectively. The initial introduction of the ONep ligand as the pendant ligand of the Ti resulted in the isolation of trinuclear species which have the general structure of $TlTi_2(\mu_3\text{-OR})_2(\mu\text{-OR})_3(OR)_4$. For **3**, the stoichiometry was significantly varied from the starting stoichiometry, and a rational synthesis of **3** was undertaken using the same starting materials but adding HOEt to generate the appropriate ligand ratio. This synthesis yielded the trinuclear product **4** (shown in Figure 4). The overall structures of **3** and **4** are identical, but the ratios of the OEt/OPr^i ligands differ. On the basis of the observed solid-state flexibility of these trinuclear complexes, it is not unreasonable to believe a wide variety of OEt and OPr^i complexes in different ratios could be (and are) synthesized in these reactions. Because of the success of the reduced nuclearity and coordination around the Tl atom, $[Tl(\mu\text{-ONep})]_\infty$[19] and $[Ti(\mu\text{-ONep})(ONep)_3]_2$[8] were used to generate the homoleptic product. For **5**, the Tl atom was found to be disordered over three sites which also leads to disorder in the attached ONep atoms. Figure 5 shows the Tl disorder over the central core of **5**. The carbons and the disorder among the oxygens are not shown for clarity. A number of crystals from different batches were investigated to improve the final structure, but the disorder was noted for each sample. While a great deal of disorder is apparent in this molecule, the trinuclear arrangement, which is consistent with **3** and **4**, was unequivocally established for **5**.

For **3**−**5**, the two Ti metal centers are bound to the lone Tl atom through two bridging μ_3-OR ligands (**3**, μ_3-OR = OEt; **4**, μ_3-OR = OEt and ONep; **5**, μ_3-OR = ONep). The Oh geometries of each Ti atom of **3**−**5** possess terminal ONep ligands. The Tl atoms are 4-coordinated, formally adopting a pyramidal (PYR) geometry but with the inclusion of the lone pair of electrons each Tl forms a SBP arrangement. This type of structure is reminiscent of the $Ti(O)_x(ORc)_y(ONep)_z$ (ORc = carboxylate ligand) species[14] and the $KZr_2(OPr^i)_9$ complex previously discussed. The K/Zr structure could not be isolated without a Lewis basic solvent bound to the K.[27] For **3**−**5**, there is no inclusion of solvent because of the free electrons of the Tl atoms that disfavor coordination of a Lewis basic solvent. For the ONep ligated

(27) Vaartstra, B. A.; Streib, W. E.; Caulton, K. G. *J. Am. Chem. Soc.* **1990**, *112*, 8593.

Table 4. Select Bond Distances (Å) and Angles (deg) for **6** and **7**

Distances (Å)

	6		**7**	
Tl···Ti	Tl(1)···Ti(1)	3.5832(6)	Tl(1)−Ti(1)	4.735
			Tl(1)−Ti(1a)	5.813
Tl−(μ-OAr)	Tl(1)−O(1)	2.545(2)		
Tl−(μ-OR)	Tl(1)−O(2)	2.600(2)		
Ti−(μ-OAr)	Ti(1)−O(1)	2.014(2)		
Ti−(μ-OR)	Ti(1)−O(2)	1.894(2)		
Ti−(OAr)	Ti(1)−O(5)	1.883(2)	Ti(1)−O(1)	1.882(4)
			Ti(1)−O(2)	1.857(4)
			Ti(1)−O(3)	1.953(4)
			Ti(1)−O(4)	1.888(4)
			Ti(1)−O(5)	1.877(4)
Ti−(OR)	Ti(1)−O(3)	1.811(2)		
	Ti(1)−O(4)	1.817(2)		

Angles (Å)

	6		**7**	
Tl−(μ-OAr)−Ti	Tl(1)−O(1)−Ti(1)	103.06(8)		
Tl−(μ-OR)−Ti	Tl(1)−O(2)−Ti(1)	104.74(8)		
(OAr)−Tl−(OR)	O(1)−Tl(1)−O(2)	59.58(6)		
(OAr)−Ti−(OR)	O(1)−Ti(1)−O(2)	81.66(8)		
(OAr)−Ti−(OAr)			O(1)−Ti(1)−O(2)	92.05(19)
			O(1)−Ti(1)−O(3)	178.0(2)
			O(1)−Ti(1)−O(4)	92.9(2)
			O(1)−Ti(1)−O(5)	89.3(2)
			O(2)−Ti(1)−O(3)	87.32(19)
			O(2)−Ti(1)−O(4)	119.5(2)
			O(2)−Ti(1)−O(5)	123.0(2)
(OAr)−Ti−(μ-OAr)	O(5)−Ti(1)−O(1)	84.08(9)		
(OAr)−Ti−(μ-OR)	O(5)−Ti(1)−O(2)	127.97(10)		
(OR)−Ti−(μ-OAr)	O(3)−Ti(1)−O(1)	93.38(9)		
	O(4)−Ti(1)−O(1)	170.89(9)		
(OR)−Ti−(μ-OR)	O(3)−Ti(1)−O(2)	112.09(10)		
	O(4)−Ti(1)−O(2)	94.04(9)		
(OR)−Ti−(OR)	O(3)−Ti(1)−O(4)	95.69(10)		
(OAr)−Ti−(OR)	O(5)−Ti(1)−O(3)	118.52(10)		
	O(5)−Ti(1)−O(4)	92.38(10)		

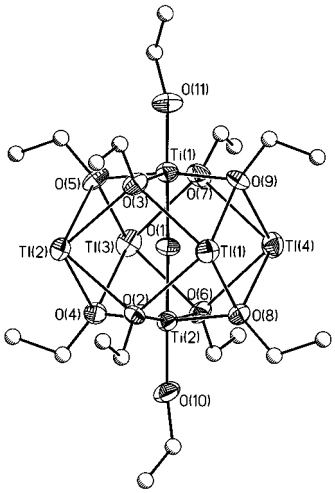

Figure 1. Thermal ellipsoid plot of **1**. Ellipsoids are drawn at 30% theoretical.

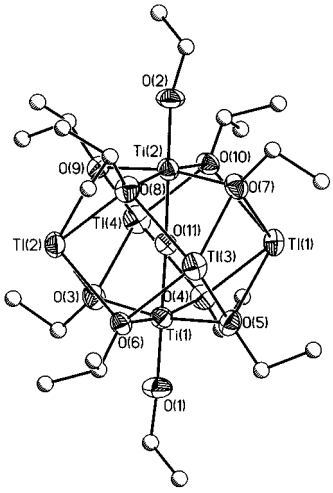

Figure 2. Thermal ellipsoid plot of **2**. Ellipsoids are drawn at 30% theoretical.

species, we have successfully reduced the coordination around the Tl atoms; however, on the basis of structural considerations, the Tl cation is still too encumbered to undergo a "clean" metathesis reaction (eq 3).

To further reduce the coordination around the Tl metal center, additional steric bulk was added to the system using the aryloxide $[Tl(\mu\text{-DMP})]_\infty$.[19] The product isolated was the dinuclear species **6** (Figure 6). The Tl and Ti are bound by a single μ-ONep and μ-OAr ligand with a combination of terminal DMP and ONep ligands filling the TBP environment around the Ti atom. The Tl atom is formally 2-coordinated in a bent geometry, but because of the presence of the free electrons, bond angles resemble a trigonal planar geometry. The analogous species, $Tl(\mu\text{-OBu}^t)_3Sn$[28] and $Li(\mu\text{-OAr}^{ph})_3$-

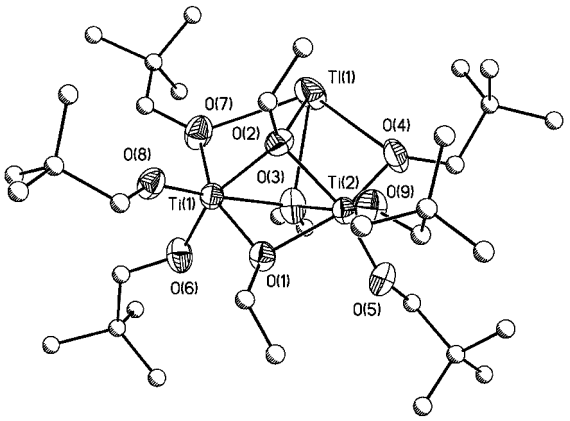

Figure 3. Thermal ellipsoid plot of **3**. Ellipsoids are drawn at 30% theoretical.

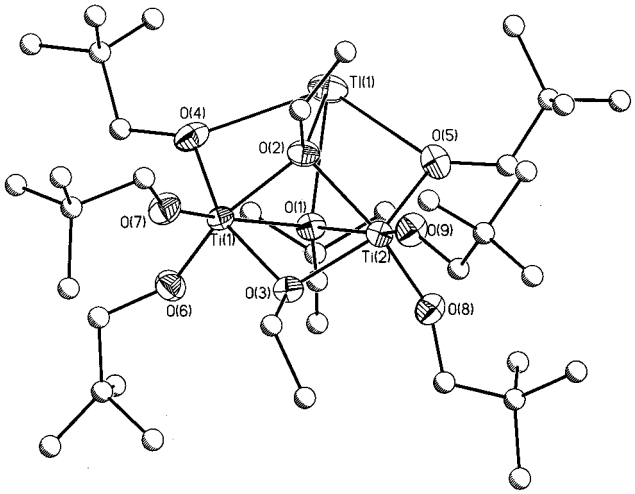

Figure 4. Thermal ellipsoid plot of **4**. Ellipsoids are drawn at 30% theoretical.

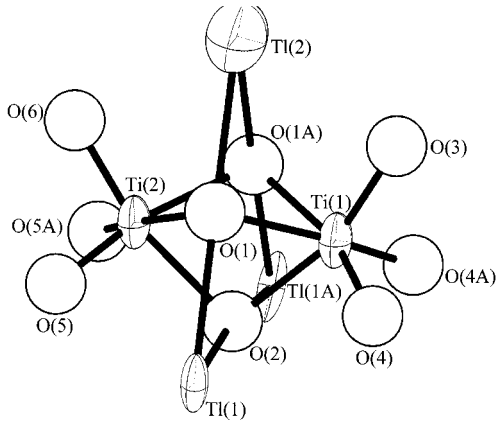

Figure 5. Plot of central core of **5** showing the disorder of the Tl atoms over the three sites. The carbons of the ONep ligands and the disorder in the oxygen atoms have been omitted for clarity. Ellipsoids are drawn at 30% theoretical.

Sn,[29] were found to adopt significantly different arrangements. The $(THF)_2Li(\mu\text{-}OR)W(OR)_4$ species[30] appears structurally similar, as do several other dinuclear compounds;[4] however, most involve the coordination of a solvent. Again, the presence of the lone pair of electrons on the Tl atoms precludes Lewis base coordination.

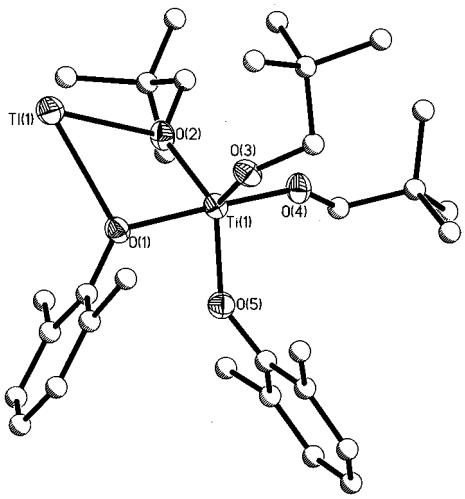

Figure 6. Thermal ellipsoid plot of **6**. Ellipsoids are drawn at 30% theoretical.

In an effort to introduce as much steric bulk as possible and thus generate the most accessible Tl, the homoleptic aryloxide species was synthesized using $[Tl(\mu\text{-}DMP)]_\infty$[19] and $Ti(DMP)_4$.[22] The resulting orange colored crystals isolated from this reaction proved to be the unique species, **7** (Figure 7). In the unit cell, the Ti metal center of the $Ti(OAr)_5^-$ moiety was found to be TBP and significantly distanced from the Tl cation (Tl···Ti = 5.584 Å), implying a fully ionic species with an unsupported Tl cation present (Figure 7a). Further study of the structure reveals an interaction of the Tl cation with four DMP π-arene electrons in an η^2 or η^3 fashion (Figure 7b). This interaction with the nearest neighbor leads to a Tl···Ti distance of 4.870 Å and a Tl−Cn (Cn = centroid) average distance of 3.45 Å. The shortest distance is between the Tl cation and one of the nearest neighbor's DMP ligands (Tl(1)−Cn(1a) = 2.592 Å). The shortest Tl−C bond distance of 2.638 Å is longer than the Tl−Cn(1a) distance because the latter is measured to the plane.

A search for intermolecular contacts between Tl···C at a distance of 2.0 and 3.0 Å in the Cambridge database led to a series of Tl···C π-interactions with cyclopentadienyl (Cp) ligands.[31−35] The Tl−C distances typically involve the Tl−Cp ring and range from 2.735 to 2.973 Å.[31−35] A Tl−π-arene interaction was observed for a Tl[9-(1-cyclopentadienyl-1-methylethyl) fluorenyl] complex.[33] In this structure, the Tl metal center is bound to a cyclopentadienyl ligand as well as the π-arene ring of the side group. The π-arene bond distance was found to be substantially longer (av 3.54 Å)

(28) Veith, M.; Rosler, R. *Angew. Chem., Int. Ed. Engl.* **1982**, *21*, 858.
(29) Smith, G. D.; Fanwick, P. E.; Rothwell, I. P. *Inorg. Chem.* **1989**, *28*, 618.
(30) Davies, J. L.; Gibson, J. F.; Skapski, A. C.; Wilkinson, G.; Wong, W. *Polyhedron* **1982**, *1*, 641.
(31) Schumann, H.; Kucht, A.; Dietrich, A.; Esser, L. *Chem. Ber.* **1990**, *123*, 1811.
(32) Schumann, H.; Kucht, H.; Kucht, A.; Gorlitz, F. H.; Dietrich, A. *Z. Naturforsch., B: Chem. Sci.* **1992**, *47*, 1241.
(33) Frank, W.; Kuhn, D.; Muller-Becker, S.; Razavi, A. *Angew. Chem., Int. Ed. Engl.* **1993**, *32*, 90.
(34) Lin, G.; Wong, W.-T. *J. Organomet. Chem.* **1995**, *495*, 203.
(35) Enders, M.; Fink, J.; Pritzkow, H. *Eur. J. Inorg. Chem.* **2000**, 1923.

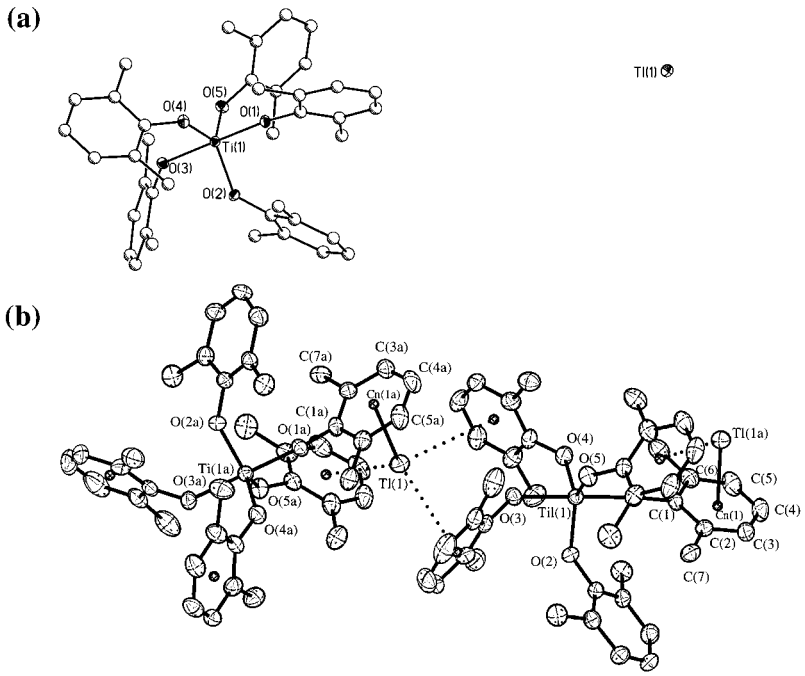

Figure 7. Thermal ellipsoid plot of **7**. Ellipsoids are drawn at 30% theoretical: (a) unit cell diagram, (b) interaction with nearest neighbor.

than the Tl−Cp interaction (av 2.86 Å). Therefore, the π-binding behavior noted for **7** is the shortest reported to date, even for the Tl−Cp interactions. This is quite unexpected because even though there is potential for a Tl−O bond formation, as noted for **6**, the Tl prefers the π-interaction. Besides being one of the first unsupported ionic metal alkoxides, **7** also has a very strong π-arene ring interaction.

Metrical Data. The significant disorder noted for the crystal structures of **3** and **5** precludes discussion of their metrical data; however, the connectivity of the molecule has been unequivocally determined. For the remaining compounds, the final structures are of high enough quality that the metrical data can be meaningfully discussed.

As is typically observed for metal alkoxides, an increase in the degree of bonding of the ligand for **1**−**2**, **4**, and **6**−**7** leads to an increase in the length of the M−O bonds. The one exception to this trend is noted for **4**: the Tl−(μ-OR) distances (av 2.73 Å) are longer than the Tl−(μ_3-OR) distances (av 2.58 Å). The anomalous distances noted may be a reflection of geometrical constraints due to the two μ_3-OR groups. The Tl···Ti distances increase as the nuclearity of the molecule and the coordination around the Tl atom decrease (av Tl···Ti: 3.43 Å, **1**; 3.44 Å, **2**; 3.52 Å, **4**; 3.58 Å, **6**; 5.27 Å, **7**). The remaining distances are in agreement with the literature values reported for $[Tl(OR)]_x$[19] and $[Ti(OR)_4]_n$.[8,20,21] For example, even with the introduction of the Tl cation, the Ti···Ti distance of **4** is not varied from the unsubstituted $[Ti(\mu\text{-ONep})(ONep)_3]_2$.[8]

Solution State. NMR. Sealed NMR samples of saturated crystalline powders of **1**−**7** in toluene-d_8 were used to collect the ^{1}H, ^{13}C, and ^{205}Tl NMR spectra to evaluate their solution behavior. Table 5 lists some of the ^{205}Tl NMR data that are correlated with aspects of the single-crystal metrical data.

If the solid-state structure of **1** is retained in solution, two types of OEt ligands should be observed, terminal and μ_3-OEt, in a 1:4 ratio. For the ^{1}H NMR spectrum of **1**, two types of methylene resonances were observed in a 1:3.5 ratio. However, further investigations using ^{13}C NMR indicated that as many as 5 types of methylene carbon atoms were present. The additional resonances may be accounted for by disruption of symmetry of the molecule (i.e., breaking of a single M−(μ_3-OR) bond). It is difficult to confirm structure retention because of the overlapping nature of the various resonances. Therefore, we decided to utilize ^{205}Tl NMR to further elucidate the solution behavior.

Table 5. Solution NMR Data an Structural Parameters for **1**−**7**

compd	^{205}Tl[a] (tol-d_8)	MC[c] (Tl/Ti)	CN[c]	Tl−O (Å) (av)
1	1506, 1503, 1486, 1477(major), 1419, 1401	2	5	μ_3-OR 2.63, μ-OR 2.85
2	2319, 2271, 2224, 1570, 1523(major), 1497, 1494, 1484	2	5	μ_3-OR 2.66, μ-OR 2.83
3	1426, 1203, 1378, 1372, 1358(major), 1332	0.5	4	NR[d]
4	1373, 1358(major), 1333	0.5	4	μ_3-OR 2.59, μ-OR 2.73
5	1406, 1380, 1374, 1360(major), 1340	0.5	4	NR
6	1453, 1427, 1405, 1395, 1379, 1364, 1359(major), 1339(major), 1333	1.0	2	μ-OAr 2.545(2), μ-OR 2.600(2)
7	2034	1.0	4	none

[a] Solution NMR referenced to 0.001 M $Tl(NO_3)$ (δ = 0.0 ppm). [b] MC = molecular complexity (number of Tl/number of Ti metal centers). [c] CN = coordination number of Tl cations. [d] NR = not reported because of quality of the crystal structure.

The chemical shifts of Tl metal centers are extremely sensitive to subtle changes in their environment.[17−19] The symmetry of **1** indicates one type of ^{205}Tl NMR resonance should be observed if the structure is retained upon dissolution. A major peak at 1479 ppm was observed for **1** with several shoulders and other minor peaks present. For this

compound, and as is often reported for other metal alkoxides, dynamic ligand exchange is expected. Because there are only OEt ligands present, any changes in the environment of the Tl must be attributed to changes in bonding such as a μ_3-OEt ligand reducing to a μ-OEt ligand. This would alter the coordination sphere slightly around several Tl atoms, and thus, this variation and ones like it may account for the smaller peaks present. Further investigations into the dynamic behavior of **1** by variable temperature NMR (VT-NMR) were not undertaken because of the thermal instability of the smaller alkoxide ligated species at higher temperatures and the propensity of **1** to crystallize at lower temperatures. The possibility of these minor peaks representing partial hydrolysis products could not be conclusively ruled out on the basis of some preliminary hydrolysis experiments conducted on these samples (initial attempts to introduce water into these systems yielded insoluble species, the mother liquor of which had no ^{203}Tl NMR signal). The preceding information indicates that there is one major component that would be consistent with the solid-state structure, but definitive claims on the solution structure await further testing.

Because of the similarity of structures, rearrangement as described for **1** should be expected for **2**; however, the mixed ligation of **2** will add further complications. The ^{1}H NMR spectrum of **2** revealed two smaller methylene resonances and one methine resonance in a 2:2:5 ratio as well as two methyl resonances which appear as one broad singlet and one doublet. The ^{13}C NMR spectrum shows one methyl resonance for the OEt and one for the OPr^i ligands and three methylene or methine carbons. This is consistent with the ^{1}H NMR spectrum indicating two types of OEt and one type of OPr^i ligands. The ^{205}Tl NMR of **2** revealed three large peaks at 1570, 1523(major), 1497 ppm. There are also several additional minor peaks present around this chemical shift. Because of the presence of two types of ligands (OEt and OPr^i), the statistical variations around a single Tl atom could range from fully OPr^i to fully OEt and the statistical variations in between. This would result in a number of new environments for the Tl metal center. Several additional ^{205}Tl resonances were also observed further downfield at 2319, 2271, and 2224 ppm. Because of the bandwidth limitations of the probe, an acceptable integration between the two resonance clusters could not be obtained. However, the resonances at 1500 ppm were the dominant resonances in the spectrum. The ^{205}Tl NMR chemical shifts reported for the parent $[Tl(OEt)]_4$ and $[Tl(OPr^i)]_4$ appear at 2914 and 3067 ppm, respectively. Therefore, **2** may be partially disrupted in solution, which must be attributed to the OPr^i ligand. Again, thermal degradation and preferential crystallization precluded VT-NMR investigations.

^{1}H and ^{13}C NMR data for **3** and **4** should be very similar because of the mixed ligand distributions in the two structures. The ^{1}H NMR spectra of both compounds show broad peaks for the OEt ligands and relatively sharp peaks for the ONep ligands. There is a great deal of overlap between the two sets of methylene and methyl resonances. The ^{13}C NMR is simplistic, revealing only a single set of resonances consistent with the OEt and ONep ligands. ^{205}Tl NMR spectra were also obtained for **3** and **4**. It is assumed, because of the similarity in mixed ligated species of **3** and **4** that are present for both species, that similar Tl environments would be present. For **3**, the major peak observed is present at δ 1358 with several minor resonances observed. For **4**, there are at least four types of Tl atoms present with a major peak present at 1347 (minor at 1376, 1369, and 1349 ppm). The Tl environments observed for **1** and **2** are further upfield, most likely a reflection of the absence of a μ_3-O in **3** or **4**. The parent $[Tl(\mu_3\text{-OEt})]_4$ and $[Tl(\mu_3\text{-ONep})]_4$ ^{205}Tl resonances appear at 2914 and 2561 ppm, respectively, arguing that total disruption of the compounds upon dissolution is not occurring. As noted for **1** and **2**, ligand redistribution will produce changes in the Tl environment. Statistically, for **3**, there are four types of Tl environments available (OEt:ONep in a ratio of 0:4, 1:3, 2:2, and 3:1), and several ^{205}Tl NMR resonances were present which may represent the more statistically valid arrangements. For **4**, three Tl environments were observed. This may be a representation of the various combinations of OEt:ONep ligands that could be observed (0:4, 1:3, and 2:2). The major resonance observed would most likely represent the statistically biased homoleptic ONep ligated environment. There are no observable Tl$\cdots$Tl splittings for either **3** or **4**, indicating that hybridized clusters containing Tl$-$O$-$Tl bonds are not formed. On the basis of the preceding ^{205}Tl NMR data, it appears that the solid-state structure is maintained for **3** and **4**; however, many environments around the Tl atoms are present because of dynamic ligand exchanges.

The solid-state structure of **5** should possess three types of ONep (4 terminal, 3 μ-, and 2 μ_3-) ligands. For the solution ^{1}H NMR spectrum of **5**, there are two broad overlapping methine and three methyl resonances in a 1.4:0.5:7.75 ratio. The solution ^{13}C NMR spectrum reveals one type of methyl, one quaternary, and two methine carbon resonances. This is consistent with bridging and terminal ligands with coincidental overlap of the remainder of the ligands. Again, ^{205}Tl NMR spectra were obtained to further elucidate solution behavior. One resonance is expected for the Tl spectrum of **5** if the solid-state structure is maintained in solution. Unlike **3** and **4**, there is only one environment that can be realized with the homoleptic species. The actual ^{205}Tl NMR spectrum reveals the presence of at least six resonances. The major resonance (by a factor >3) resides at δ 1360 ppm. Three other minor resonances appear around 1380 ppm with several trace resonances also present. None of these resonances correspond to the parent $[Tl(ONep)]_4$ resonance which was found at 2561 ppm. The steric bulk of the ONep versus the OEt and OPr^i ligands is increased enough to yield smaller ligated species in other systems.[7−14] Therefore, with an all ONep ligated complex, disruption of the trinuclear species to yield smaller dinuclear species (i.e., "$Tl(\mu\text{-ONep})_2Ti(ONep)_3$" or "$Tl(\mu\text{-ONep})_3Ti(ONep)_2$") should be accessible and may explain some of the new Tl environments observed. If this were so, the Tl shift of **5** and **6** should be similar despite the pendant groups, as has been observed (vide infra).

Mixed ligated species **6** is asymmetric and should reveal multiple resonances. The ^{1}H and ^{13}C NMR spectra of **6** reveal

only one set of resonances for the ONep and OAr ligands. This is most likely due to coincidental overlap or rapid exchange of the terminal and bridging ligands. The ^{205}Tl NMR spectrum has several major resonances at 1347 (major), 1332, and 1324 and several minor resonances. As observed for any of the mixed ligated species, multiple Tl environments should be observed because of ligand rearrangement. Full dissociation does not occur because there are no chemical shifts around 2000 ppm as noted for **3** and **7**.

For **7**, the solid-state structure has a single Tl atom but two types of DMP ligand because of the asymmetric π-interaction of the Tl cation. The ^{1}H and ^{13}C of **7** revealed only a single set of DMP resonances which implies an averaging of the Tl$-\pi$-ring interaction in solution. The ^{205}Tl chemical shift of the $[Tl(OAr)]_\infty$ (OAr = DMP, DIP) polymers which reportedly were monomeric in solution had resonances at 1999 and 1850 ppm, respectively. On the other hand, the cubic structures of $[Tl(OR)]_4$ had resonances that ranged from 2500 to 3200 ppm. Therefore, it was assumed that ionic-like Tl cations should appear around 2000 ppm; however, this may also be a shielding effect by lying between four π-arene rings. The ^{205}Tl NMR spectrum revealed a broad signal at δ 2035 which implies that **7** has an ionic nature which is not unreasonable because of the charge separation noted for the solid-state structure. This is also significantly shifted from the covalently bound Tl species **1**$-$**6** which typically had multiple signals around 1500 ppm. The ^{205}Tl chemical shift of ionic, Tl species are often strongly influenced by the solvent and/or concentration effects.[17−19] Few changes were noted for concentration-varied samples of **7**. The π-interaction between the Tl and the $Ti(OAr)_5$ is strong enough to remain intact independent of any external influences.

A comparison of the ^{205}Tl shifts to the coordination number (see Table 5) indicates that there is a correlation between the chemical shift observed and the geometry in which the cation is located: for 5-coordinated alkoxy oxo species, the resonances appear in the high 1400 and low 1500 ppm range, for 4 coordinated, the mid 1300 ppm range, and for the 2-coordinated, the low to mid 1300 ppm range. As shown in Table 5, there does not appear to be any correlation between bond distances and the resultant ^{205}Tl chemical shift. While this is a general pattern that can be used to aid in the identification of mixed alkoxide Tl species, a much larger database is necessary to fully verify this trend.

Summary and Conclusion

A new family of structurally diverse compounds has been characterized by single-crystal X-ray diffraction as $Tl_4Ti_2(\mu\text{-}O)(\mu_3\text{-}OEt)_8(OEt)_2$ (**1**) and $Tl_4Ti_2(\mu\text{-}O)(\mu_3\text{-}OPr^i)_5(OEt)_5$ (**2**), and $TlTi_2(\mu_3\text{-}OEt)_2(\mu\text{-}OEt)(\mu\text{-}ONep)_2(ONep)_4$ (**3**), $TlTi_2(\mu_3\text{-}OEt)(\mu_3\text{-}ONep)(\mu\text{-}OEt)(\mu\text{-}ONep)_2(ONep)_4$ (**4**), $TlTi_2(\mu_3\text{-}ONep)_2(\mu\text{-}ONep)_3(ONep)_4$ (**5**), $TlTi(\mu\text{-}DMP)(\mu\text{-}ONep)(DMP)(ONep)_2$ (**6**), and $[Tl^+][^-(\eta^{2-3}\text{-}DMP)Ti(DMP)_4]$ (**7**). The coordination of the Tl cation for the $TlTi(OR)_5$ family of compounds can be systematically decreased through the introduction of increasingly sterically demanding ligands. The most hindered species yielded the unique $[Tl^+][^-(\eta^{2-3}\text{-}DMP)Ti(DMP)_4]$ molecule. This is the first unsupported ionic metal alkoxide observed to date and displays an unusually strong π-interaction.

Solution ^{205}Tl NMR data proved to be the most useful means to study the solution behavior of the crystalline material. These data indicate that the major portion of the solution state structures of **1**$-$**7** are in agreement with the solid-state structures; however, a great deal of ligand exchange occurs, yielding several Tl environments. In general, the covalently bound Tl$-$Ti double alkoxide compounds have ^{205}Tl NMR chemical shifts that appear at ∼1500 ppm, whereas the ionic $TlTi(OR)_5$ species (**7**) revealed a single resonance at ∼2000 ppm. The trend observed here is the reverse of what was observed for the Tl only species (ionic species were at ∼2000 ppm and covalent cubes were at ∼2500 ppm).[19] The covalently bound Tl$-$Ti species are ∼1000 ppm upfield in comparison to the $[Tl(OR)]_x$ compounds. The increased number of alkoxide and oxo ligands bound to the Tl metal centers increases the amount of electron donation, which increases the shielding of the metal centers, moving the resonances upfield. One convenient method for discussing these compounds is to define the molecular complexity as a ratio of Tl atoms to that of the number of Ti atoms. The introduction of more $\delta+$ Ti metal centers coupled with a reduction in the number of electron donating oxygen bearing ligands results in an upfield shift of the resonances. In contrast, the ionic species of the $[Tl(OAr)]_\infty$ polymer and **7** appear in the same region.

By slowly increasing the steric bulk of the pendant hydrocarbon chains of the alkoxide ligands, we have systematically altered the original cluster structures noted for the lower alkoxide ligands to a fully ionic species using the bulky aryloxide ligands. The fine-tuning of the Tl$-$Ti double alkoxide system has allowed for control over the degree of accessibility of the Tl cation for use in future metathesis reactions. Initial investigations indicate that only the Tl cation of **7** is sufficiently accessible to initiate metathesis reactions.

Acknowledgment. For support of this research, the authors would like to thank the United States Department of Energy under Contract DE-AC04-94AL85000. Sandia is a multiprogram laboratory operated by Sandia Corporation, a Lockheed Martin Company, for the United States Department of Energy.

Supporting Information Available: One X-ray crystallographic file, in CIF format, is available for **1**$-$**7**. This material is available free of charge via the Internet at http://pubs.acs.org.

IC0110833